Flashback-induced flame shape transition in a two-stage LPP aeronautical combustor

Léo C.C. Mesquita, Aymeric Vié, Sébastien Ducruix

Flashback-induced flame shape transition in a two-stage LPP aeronautical combustor

Léo C. C. Mesquita[a], Aymeric Vié[a,*], Sébastien Ducruix[a]

[a] *Laboratoire EM2C, CNRS, CentraleSupélec, Université Paris-Saclay, 3 rue Joliot Curie, 91190 Gif-sur-Yvette, France*
∗ *Corresponding author: aymeric.vie@centralesupelec.fr*

Abstract

Large-Eddy Simulations were performed to study the flashback-induced flame shape transition of a lean premixed M flame in a staged liquid-fuelled aeronautical lean-burner, as observed experimentally. The BIMER combustor is a Lean Premixed Prevapourised (LPP) burner composed of two stages, each with its own injector and swirler: the main outer stage, called multipoint, uses jet-in-crossflow injection to achieve the LPP regime, while the central stage, called pilot, uses a pressure swirl injector to create a hollow cone spray to stabilise the flame. During LPP operation, this M flame presents a strong acoustic activity, promoting a periodic flashback of its leading edge. When, aiming to stabilise the flame, the pilot injection is increased and the multipoint injection decreased, the oscillating leading edge (due to the longitudinal acoustic perturbations) attaches to the pilot spray, changing the flame into a Tulip shape. Two phenomena were identified as being the most relevant causes of this flame shape transition. First, the leading edge position and the thermoacoustic instability amplitude are directly linked to the combustion chamber final temperature. The higher the temperature in the chamber, the more upstream the leading edge stabilises and the higher the acoustic oscillation amplitude, increasing the risk of a successful flashback. Second, the injection regime with high pilot injection allows the leading edge to attach to the pilot spray, as the flame only reattaches when the pilot spray is sufficiently high. The higher the pilot fuel flow, the higher the amount of fuel sprayed in the critical region where the flame might attach for a transition to the Tulip shape. Therefore, as the change in injection regime is the main mechanism lean staged burners use to reduce emissions while increasing operability, this works shows that an M flame is unsuitable to such burners with similar aerodynamic topology and properties.

Keywords: Lean Premixed Prevapourised; Large-Eddy Simulations; Flashback; Bifurcation, Staged combustion . . . (8/10)

1. Introduction

Lean Premixed Prevaporized (LPP) burners aim at a more efficient and cleaner combustion by targeting a lean and homogeneous mixture, reducing temperature and nitrogen oxides. However, LPP regimes are prone to unstable behaviours [1, 2], as lean extinction, flashback or thermoacoustic instabilities. Staged injection, which can control the flame behaviour by splitting the fuel supply in several swirler and injector stages, is currently being investigated as a viable strategy to stabilise the combustion in LPP regime [3]. The two-stage BIMER combustor has been designed at the EM2C laboratory aiming to further study and develop this type of burner. It is composed of a central pilot stage, which uses a pressure-swirl injector to sustain a spray diffusion-like pilot flame, and an outer swirl stage, which uses multi-point injection to generate the LPP mixture and flame inside the chamber [4].

Experimental and numerical studies have shown that three flame archetypes can be stabilised in this burner: a V flame, an M flame and a Tulip flame [4, 5]. Three flame shape bifurcations can be triggered by a change in the the distribution of fuel between the two stages [4, 6, 7]. Between these flames, the M one is a premixed lifted flame, thus showing optimal properties in terms of a clean combustion. However, in [4] the authors have observed a flashback of the lifted flame while increasing fuel from the pilot injector, which is the designed manoeuvre of staged burners to reduce flame dynamics and instabilities [3]. The M flame then reattaches to the pilot spray and transitions to a Tulip shape, a diffusion-like and potentially highly-polluting flame. This transition is clearly undesirable, as it changes a clean premixed flame into a source of pollutant emissions, nullifying the use of an LPP system. Furthermore, it happens when the pilot stage is activated with the objective of stabilising the system, thus also nullifying this action of the staged injection technology. Moreover, even if there are other studies in the literature about flashback in staged burners [8, 9], they only focus on gaseous premixed systems, which neglect important phenomena such as liquid injection regime. Therefore, the purpose of this work is to investigate further this M to Tulip flame shape transition on the BIMER combustor and to shed light on the mechanisms leading to the flashback and the flame reattachment to the pilot spray in this LPP burner.

This paper is organized as follows. First, the BIMER rig is described, and the operating conditions are presented. Then, the numerical setup is characterized. Finally, the numerical simulations of the transition results are presented, compared with experiments and analysed.

2. Description of the setup

2.1. Experimental setup and operating conditions

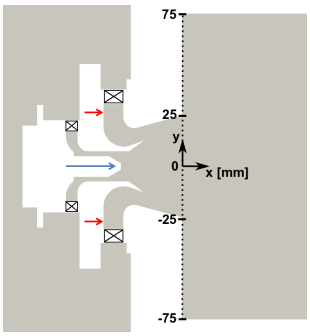

Fig. 1: 2D view of the injector at the entrance of the combustion chamber. The central blue arrow indicates the pilot injector, while the two external red arrows, the radial position of multi-point injection holes. Flow from left to right.

As mentioned, the BIMER combustor was designed to study the operation of a swirling lean-burn two-stage injector. The rig is composed by a cylindrical plenum and a rectangular combustion chamber ($500 \times 150 \times 150 mm^3$). Three of the combustion chamber walls are water-cooled (entrance, top and bottom) and the two lateral ones are silica windows for optical access. The injector is composed of two swirling stages (Fig. 1): at the centre is the pilot stage, where 15 % of the total air mass flow rate goes through and that uses a pressurized nozzle to create a fuel spray with a hollow cone shape and a spray half angle of 30°. This stage swirler has a geometric swirl number of 0.6. The outer and main stage, where 85 % of the air mass flows, is called the multi-point stage, as its injector uses 10 holes of 0.3 mm diameter placed at the swirler exits to create a jet in cross-flow injection and improve mixing. This stage swirler is characterized by a geometric swirl number of 1.

The burner is operated at atmospheric pressure, with preheated air at 433K, a total air mass flow rate of $43\ g\ s^{-1}$, a total fuel mass flow rate of $1.64\ g\ s^{-1}$, resulting in a global equivalence ratio of 0.6, and a thermal power of $\approx$ 73 kW. During this study, the aforementioned global parameters are constant. The staged burner technology relies on changing the fuel distribution between the stages to change the flame behaviour. This study explores such variation and the impact on the flame. The fuel distribution between stages characterised by the staging factor α, that equals the ratio between the pilot fuel mass flow rate over the total fuel mass flow rate in percent. Here, the staging factor is increased from 15% to 20%, matching the experiments of Renaud [4] (as well as all other parameters).

2.2. Numerical setup

The LES is performed using the AVBP code, co-developed by CERFACS and IFPEN [10]. The WALE model [11] is used to model the LES sub-grid scales. A Two-step Taylor-Galerkin (TTGC) scheme (3^{rd}

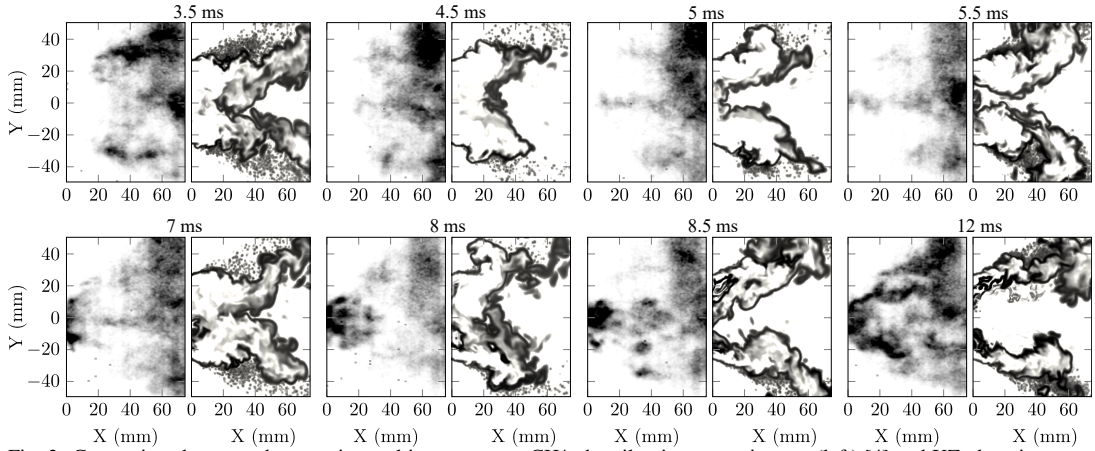

Fig. 2: Comparison between the experimental instantaneous CH* chemiluminescence images (left) [4] and XZ plane instantaneous snapshots from the LES of heat release rate (right) at the same time instants during the first step of the M to Tulip flame shape transition.

order in space and time) is used.The Navier-Stokes Characteristic Boundary Conditions (NSCBC) [12] are used to impose the gaseous inlet and outlet boundary conditions. Walls are considered as adiabatic, as no experimental measurement of the wall temperatures was available, and non-slipping.

The liquid phase is modelled using a lagrangian framework, where one numerical parcel represents one physical droplet. The Abramzon-Sirignano model [13] is used to model droplet evaporation. The interaction between droplets and the walls are modelled as a slip-only condition, where droplets slip on the wall to approximate a film-like behaviour. The injected droplet properties (i.e. velocity, diameter distribution) have been extracted from experimental studies of Renaud [4] and the injected PDFs correspond to the measurements. This injection setup has been compared to the experiments and validated in a dedicated study in [14]. Due to the absence of measurements for different staging values, the diameter distribution is considered constant and the velocity is scaled according to the fuel mass flow rate. The BFER reduced scheme [15] is used to model the chemistry, assuming a unity Lewis number, coupled to the Thickened Flame (TFLES) [16] combustion model, where the Charlette's efficiency function [17] is used to calculate the flame wrinkling and the flame-turbulence interaction. An unstructured tetrahedra mesh of 132 million elements is used, which keeps the flame thickening factor between 3 and 7.

2.3. Initialisation procedure

In [4], this transition is triggered by a change in the staging factor. From the stable M flame at $\alpha = 15\%$, the staging factor is progressively increased and when reaching values around $\alpha = 20\%$, the M flame reattaches. Here, the same procedure as [4] is reproduced numerically to simulate the flame reattachment. First, the M flame at stable $\alpha = 15\%$ is simulated and validated against numerical data from [4]. Afterwards, α is progressively increased at the rate of 1% per ms. The initial $t = 0$ ms is defined as the moment when the staging factor starts being changed.

3. Results

3.1. Reattachment of the flame

Figure 2 shows the key instants of the reattachment of the flame comparing the instantaneous CH* chemiluminescence images acquired in [4] with the XZ cut of heat release rate instantaneous snapshots extracted from the LES. The cut was preferred in comparison to an integrated image to improve the visualisation of the flame movement. At first, one can clearly observe the M-shaped flame ($t = 3.5\,\mathrm{ms}$). Both experimental and numerical results highlight the flame presence over the Outer Shear Layer (OSL), where droplets concentrate due to their interaction with the divergent walls, and on the centre line, characterised by the flame leading edge. Nonetheless, in the experiments, the branches of the flame that are stabilised over the OSL seem to be completely lifted, while this portion of the numerical flame is attached to the edges of the divergent. The second instant ($t = 4.5\,\mathrm{ms}$) shows the leading edge of the flame flashbacking at position $x = 20\mathrm{mm}$, while the outer portions of the flame move downstream. Then, the leading edge moves further upstream, reaching the edges of the divergent ($t = 5\,\mathrm{ms}$) and consequently entering it ($t = 5.5\,\mathrm{ms}$), while the outer portions of the flame continue to move downstream. In the following snapshots, a new and independent portion of flame is ignited inside the divergent ($t = 7\,\mathrm{ms}$) by the flashback of the leading edge. It starts then to propagate downstream ($t = 8\,\mathrm{ms}$) while, apparently independently, the outer portions of the flame move downstream again. The next image ($t = 8.5\,\mathrm{ms}$) shows the

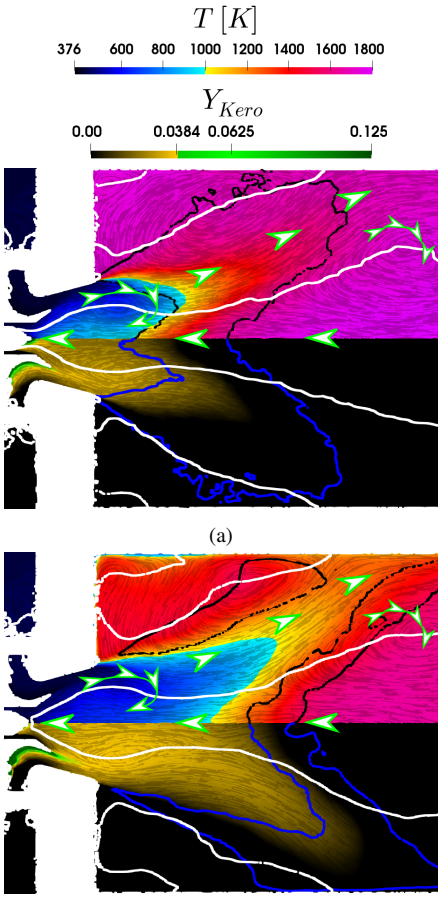

Fig. 3: XZ plane time averaged fields of temperature (top) and kerosene mass fraction (bottom), clipped to fit in the limits $[0\ ;\ 2 \times Y_{stoich} = 0.125]$ and stressing $Y_{\phi=0.6} = 0.0384$, for the (a) adiabatic and (b) isotherm walls condition. The iso-contour of zero axial velocity is shown in white lines in all images, highlighting the recirculation zones.The iso-contour of Heat Release Rate $HRR = 3 \times 10^7\ \mathrm{W/m^3}$ is shown in black on the top half and in blue in the bottom half of images. In both images the pseudo-streamlines are shown to highlight the flow path (highlighted by the green arrows) and the vortical structures, in particular the CRZ toroidal vortex.

instant when the newly ignited flame inside the divergent merges with the leading edge of the M flame and start uniting. This forms the final flame, which has a Tulip shape ($t = 12\,\mathrm{ms}$). This instant seems particularly well captured by the LES, as the inner branches of the flame around the Inner Shear Layer (ISL) and the Central Recirculation Zone (CRZ) highlight the stabilisation of this flame around the bubble of the Bubble Vortex Breakdown (BVB) topology. Also, the persistence of the outer branches of the flame stabilised over the OSL, similarly to the one observed for the M flame at $t = 3.5\,\mathrm{ms}$, supports the idea that the tulip flame is actually an M flame with its leading edge attached to the pilot spray. In opposition to the M flame, that is lean and premixed, the Tulip one is attached to the spray, burning in a diffusion-like regime. Thus, the Tulip flame produces very hot temperature inside the CRZ bubble, very likely being more pollutant than the M one [18]. Furthermore, the Tulip flame is as acoustically active as the M one, showing no gain in stability either. Therefore, avoiding this transition is essential to allow the burner to operate in lean regimes, as it is intended for this type of technology.

This comparison between experimental and numerical results shows that the LES captures very well the main events of the transition and can be used as a powerful tool to give more insight on the mechanism controlling this transition. In the following sections the most relevant phenomena leading to this transition are analysed.

3.2. M flame leading edge position

As illustrated in Fig. 2, the leading edge of the M flame plays a central role on the triggering of this transition. Thus, understanding its stabilisation process is essential to the transition analysis. In the BIMER combustor, the M flame is stabilised by a Bubble Vortex Breakdown (BVB) [19], which creates a CRZ with two parts. Upstream, an axisymmetric bubble is created by the high swirl, then, after a contraction behind the bubble, the CRZ shows a radially diverging shape. In this flow topology, the CRZ bubble is a toroidal vortex (the time-averaged flow pseudo-streamlines in Fig. 3a show that in the average flow the CRZ is an asymmetric toroidal vortex) that is in depression compared to the swirling flow [7]. These two elements attract part of the cold fresh mixture inside the CRZ bubble [7], much reducing the temperature inside the bubble when compared to the rest of the CRZ, filled with hot combustion products (the flow path is shown by the pseudo-streamlines and green arrows in Fig. 3a). While the outer parts of the M flame are stabilised over the OSL, the stabilisation of its leading edge inside the CRZ is determined precisely by the flow topology. The leading edge stabilises itself between the bubble and diverging CRZ, separating then CRZ in two zones, a Cold CRZ (CCRZ - blue regions in Fig. 3) before the flame and a Hot CRZ (HCRZ - yellow to pink regions in Fig. 3), behind the flame. Finally, it is the mix of burnt and fresh gases inside the CRZ and the consequent final temperature in this mixing zone that determines the axial position of the leading edge of the M flame.

To further explore this influence of the flow temperature on the M flame stabilisation, we study it in a second wall conditions with heat losses. This is done by considering the top and bottom walls of the chamber (intended to be water-cooled) at $100^{\circ}\mathrm{C}$, which is a rough estimation based on the experimental data of a cold wall condition. Figure 3 compares the M flame with adiabatic walls (Fig. 3a) and with heat

losses (Fig. 3b). The main differences between the two cases are the higher equilibrium temperature inside the combustion chamber for the adiabatic case and, consequently, the position of the leading edge. As shown in Fig. 3, the higher the temperature, the more upstream the M flame leading edge is. This feature is so important in this case that moving the leading edge downstream by reducing the walls temperature prevents the transition from happening. This shows that the warmer walls, achieved in this case by the adiabatic conditions, are necessary to reproduce the experiments properly and to capture transition. In the adiabatic case, the temperatures inside the HCRZ and CCRZ are higher, placing the leading edge inside the CRZ bubble, at the centre of the CRZ toroidal vortex. This region presents the highest negative axial velocity inside the bubble, which will strongly favour the flashback of the leading edge.

3.3. Self-sustained oscillations and periodic flashbacks

Figure 4 shows the evolution in time of the integrated heat release rate inside the chamber and the pressure measured near the wall at half its length, along with the flame leading edge position and axial velocity, all measured from the LES. The pressure signal from the LES was also compared to the experiments showing that the LES captures very well the frequency of the quarter-wave mode $f_{\lambda/4} \approx 300$ Hz as identified by [4]. Looking at Fig. 4, one can clearly see that this operating point is unstable and that strong self-sustained oscillations are taking place.

This is caused by the thermoacoustic coupling between the flame and the longitudinal quarter-wave mode [4]. In this case, as we will see, the major triggering mechanism of the instability is the fluctuation in fuel equivalence ratio that reaches the flame. This known mechanism [1, 2] happens here because most of the fuel comes from small droplets ($SMD \approx 15\ \mu$m) of the multipoint injection that, in their majority, evaporate and mix with the incoming air before burning, with only a small portion of droplets, with a small diameter, reaching the flame. The flow oscillations create fuel-rich pockets that modulate this mixing upstream of the flame (equivalence ratio oscillations). This causes heat release rate fluctuations in the flame that generate strong acoustic waves, further disturbing the flow, thus closing the feedback loop. In this situation, the acoustic waves strongly alters the axial velocity of the flow. The M flame leading edge then moves up- and downstream following the passage of the acoustic waves, as the flow axial velocity inside the CRZ becomes either more negative or positive when the amplitude of the axial acoustic velocity becomes higher than the local convective one and its direction is opposite. Analysing Fig. 4, one can see that the flashback instants - defined here as the instants when the flame leading edge gets inside the divergent (i.e. the leading edge has a negative axial position) - always occur following a pressure trough, moment that precedes the minimum axial velocity value inside the CRZ. This is a case of combustion instability triggered flashback [2, 20], as the leading edge is pushed upstream as a consequence of the acoustic wave passage, as also observed in [9]. Both the experimental and numerical results shown in Fig. 2 corroborate this conclusion, as the visible coordinated motion of the leading edge moving upstream, while the outer portions of the flame move downstream, is characteristic of this type of premixed flame being subject to acoustic modulations ([2, 21]). As shown in Fig. 4.a, the amplitude of oscillations is considerably higher for the adiabatic case, showing that a second effect of increasing the walls temperature is the increase in the amplitude of pressure oscillations. With higher pressure waves, the negative velocity inside the CRZ is made more negative by the passing waves, strongly increasing the chance of flashback (as described by [2]). Indeed, considering the wall heat losses during the simulations prevented the reattachment of the flame for two reasons: 1) the stable position of the leading edge was further downstream; 2) the oscillations were smaller both when compared to the adiabatic case. Additionally, the injection regime and the flow topology are the second necessary ingredient to trigger this flame transition. Both are addressed in the next section.

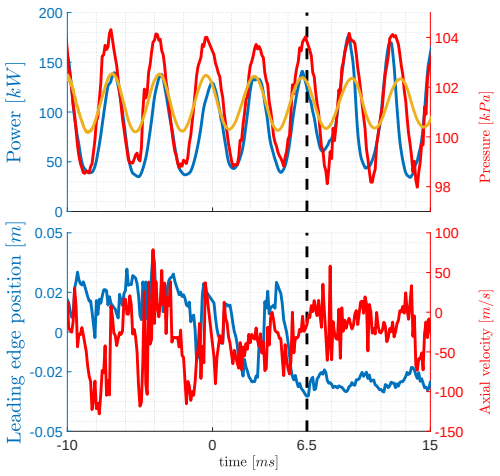

Fig. 4: Top: time evolution of the integrated heat release rate (blue) and pressure (adiabatic walls - red, isotherm walls - yellow) measured by a probe at the microphone position at $(x, y, z) = [0.25, 0, 0.075]$ m. Bottom: time evolution of the flame leading edge axial position (blue) and velocity (red). Time instant $t = 0$ ms indicates when the staging factor starts being modified and the dashed vertical line indicates the moment when the flame anchors.

3.4. Spatio-temporal fuel segregation and flow topology

The change in axial velocity amplitude as a consequence of the propagation of the acoustic waves is

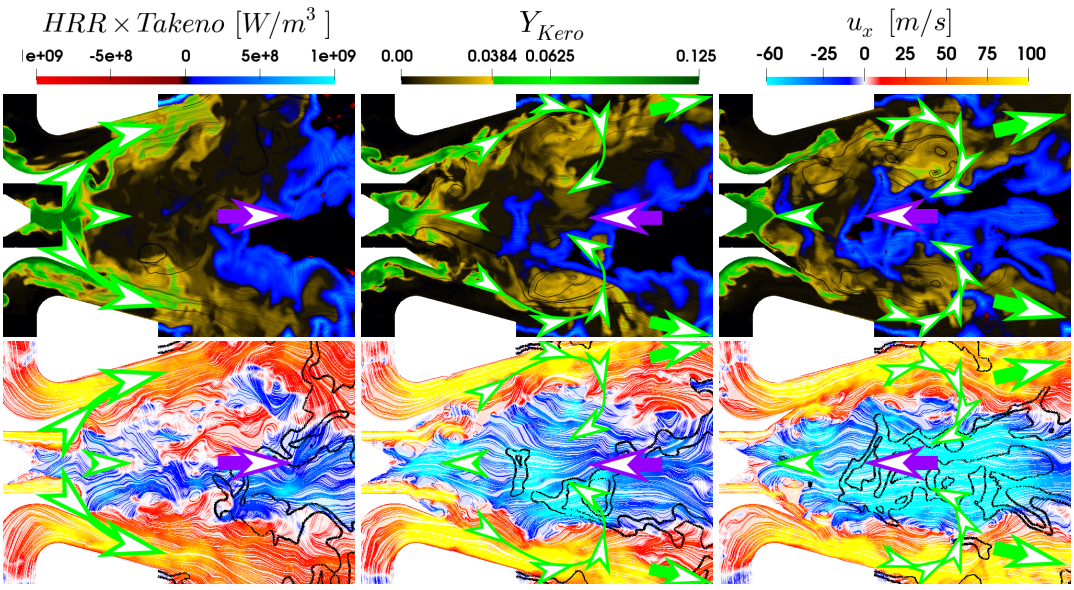

(a) t = 1.0 ms (b) t = 1.5 ms (c) t = 2.0 ms

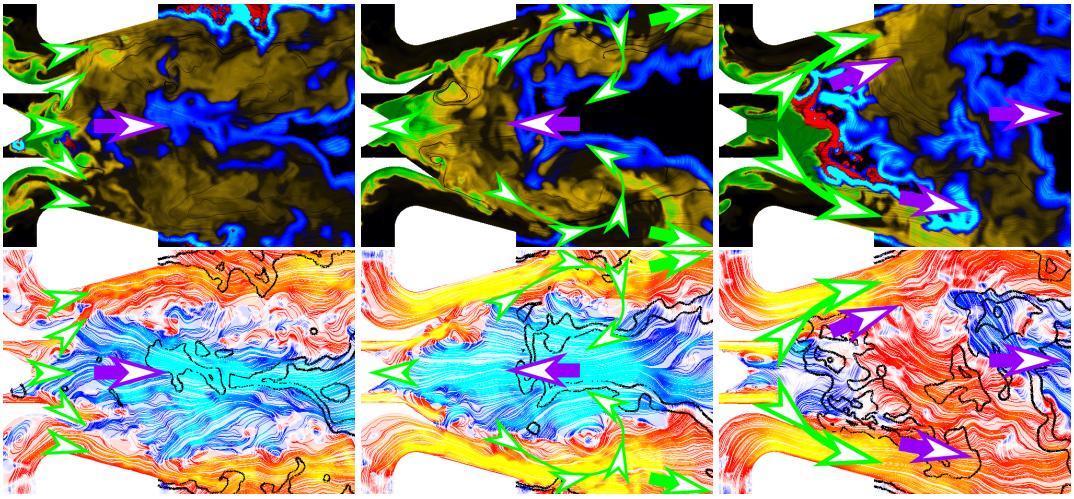

(d) t = 3.0 ms (e) t = 5.0 ms:α reaches 20% (f) t = 7.5 ms

Fig. 5: Instantaneous XZ plane snapshots of two flashbacks. Top: 2D pseudo-streamlines coloured by kerosene mass fraction (clipped to fit in the limits $[0\ ;\ 2 \times Y_{stoich} = 0.125]$ and stressing $Y_{\phi=0.6} = 0.0384$) with superimposed the product of absolute Heat Release Rate and the Takeno index $|HRR| \times TI = |HRR| \cdot \nabla Y_{Kero} \cdot \nabla Y_{O_2} / \left| \nabla Y_{Kero} \cdot \nabla Y_{O_2} \right|$ (clipped to fit in the limits $[-10^9; 10^9]\ \mathrm{W/m^3}$). Bottom: 2D pseudo-streamlines coloured by axial velocity (the CRZ is shown in blue) with heat release rate $10^8\ \mathrm{W/m^3}$ iso-contour in black. Green arrows represent the fuel movement, while the purple ones represent the flame movement.

not the sole phenomenon involved in this flame flashback. As already discussed, the M flame is stabilised over a BVB topology and its leading edge is stabilised just after the entry of fresh gases inside the CRZ bubble. Thus, the acoustic waves also affect the entire flow topology and, of particular interest in this analysis, the fuel flow and its spatial distribution in time. In comparison with flashback studies with gaseous fuel [8, 9], this aspect constitutes the main novelty, as the liquid fuel injection and dynamics play a major role in reattaching the flame and changing its shape, as we will see.

During stable operation, the BVB flow topology naturally brings part of the fuel inside the CRZ, but this creates a mixture that is too lean to be ignited. The passage of the acoustic waves creates an oscil-

lation of the fuel flow and this effect, summed with the BVB flow topology, creates a spatio-temporal fuel segregation. Figure 5 shows such a cycle, illustrating the spatio-temporal evolution of fuel and its interaction with the flow topology in two successive cycles that will first fail and then succeed in leading to a flame transition. As the axial velocity of the flow starts increasing, this also creates a wave of high fuel concentration, convected downstream by the flow, as shown by the green arrows in Fig. 5a. At this moment, the flame leading edge is also pushed downstream by the flow. As the pressure wave moves downstream, this increase in axial velocity also affects the bubble, increasing momentarily the flow rate of fresh gases entering the bubble. This is caused by the CRZ toroidal vortex (made visible by the average streamlines in Fig. 3), which pushes a wave of high fuel concentration inside the CRZ more intensely due to the passage of the pressure wave and axial velocity increase (Fig. 5b). Thus, a mixture richer than what is normally present inside the bubble is created by this effect. This increase in fuel mass fraction inside the bubble happens simultaneously as the leading edge of the flame is pushed upstream by the axial velocity inside the CRZ becoming more negative due to the passage of the pressure wave, as shown by the axial velocity contours in Figs. 5a, 5b and 5c. As the flame moves upstream, more fuel goes inside the bubble, feeding the flame from behind and sustaining it in this further upstream position for a while (Fig. 5c). This allows the flame leading edge to get closer to the pilot spray and the rich fuel mixture stocked just downstream of the pilot injector, but barely reaching it. Indeed, at this instant the staging factor (and thus the pilot fuel flow and its penetration inside the CRZ) was not high enough for the leading edge to anchor itself at the pilot spray, despite causing a local ignition of the mixture, that later extinguishes (Fig. 5d). The leading edge, then, moves back downstream as a new cycle starts and the passage of the following pressure wave reduces the amplitude of negative velocity inside the CRZ.

The following cycle starts in a similar way as the previous one. However, at the beginning of this cycle, the change in staging factor is half way through the prescribed change (Fig. 5d: $\alpha = 18.5\%$). This means that the pilot fuel flow rate is higher than for the last cycle and will progressively increase while the flame is moving as a consequence of the thermoacoustic instability. In the BVB flow topology, the majority of the pilot flow recirculates inside the bubble. The progressive increase in pilot fuel flow, thus, tends to increase the quantity of fuel that is convected inside the bubble by the self-sustained oscillations instability. At the same time, an increase in pilot fuel flow rate increases the penetration of spray and the rich evaporated fuel zone inside the CRZ bubble. Therefore, the increase in staging factor favours the flashback of the flame in these two aspects. Indeed, as the flame leading edge starts moving upstream, the change in staging factor is practically finished and the staging factor has reached the $\alpha = 20\%$ value just before the flame leading edge enters the divergent (Fig. 5e). We also see in this instant the CRZ toroidal vortex both pushing fuel inside the CRZ and accelerating the flame upstream. This increase in pilot fuel flow extends further downstream the rich mixture zone allowing more of the flashbacking leading edge to reach this region. Thus, with the higher pilot fuel flow rate corresponding to staging factor $\alpha = 20\%$, the flame leading edge ignites the fuel mixture around the pilot spray and an independent flame stabilises anchored at the spray (Fig. 5f). As the M flame leading edge moves back downstream as a consequence of the instability cycle, the newly-ignited pilot flame propagates downstream.

To understand better this flame ignition and anchoring step, Fig. 6 shows the evolution of the flame leading edge position, along with the position of iso-contours representing lean ($Y_{fuel_{\phi=0.5}}$), global ($Y_{fuel_{\phi=0.6}}$) and stoichiometric ($Y_{fuel_{stoich}}$) fuel mass fraction. This graph further supports the previous discussion on how the combustion instability interaction with the flow topology provides the fuel necessary for the flame to flashback. Just after the flame reaches its downstream-most position (meaning that the fuel is about to enter the CRZ bubble, as shown in Fig. 5) the mixture at the leading edge location becomes richer. This fuel movement immediately precedes each flame flashback, feeding the flame and allowing it to move upstream. However, when analysing the axial oscillation of the stoichiometric fuel mass fraction (Fig. 6: top red line graph) one can see that it oscillates in phase with the leading edge. This means that, as the leading edge moves upstream, also does the stoichiometric and rich fuel mixture regions, preventing the leading edge from igniting this mixture. Indeed, in all the flashbacks before the start of the staging factor modification (i.e. before $t = 0\,\mathrm{ms}$) and particularly the one at $t = -1\,\mathrm{ms}$, the leading edge does not reach the stoichiometric mixture region. When increasing the staging factor, though, the flame leading edge is able to reach the stoichiometric region at $t \approx 3\,\mathrm{ms}$, as shown in Fig. 6. Thus, during the first flashback presented in Fig. 5d the leading edge reaches the stoichiometric zone and, as shown by the spike in temperature in the same graph, it was able to ignite the mixture momentarily. Nevertheless, a flame could not be stabilised because the staging factor was still too low, meaning the mixture reached by the bulk of the flame was still too upstream and too lean. In the following flashback (shown in Fig. 5e), however, when the flame moves upstream the stoichiometric region is located more downstream than during the previous cycle, as the staging factor is already $\alpha = 20\%$. Again as the flame leading edge moves upstream, so does the stoichiometric mixture region, but as now the pilot fuel flow rate is higher, the stoichiometric region travels further downstream and the less back, upstream. This difference makes the flame leading edge meet the stoichiometric region in a more downstream posi-

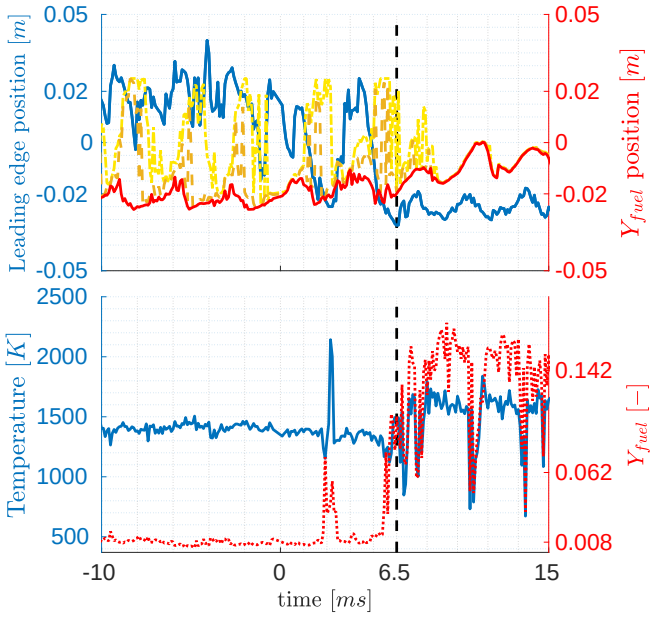

Fig. 6: Top: time evolution of the axial position of the flame leading edge (blue), the iso-contour of $Y_{fuel_{\phi=0.5}} = 0.0322$ (bright yellow), the iso-contour of $Y_{fuel_{\phi=0.6}} = 0.0384$ (orange) and the iso-contour of $Y_{fuel_{stoich}} = 0.0625$ (red). Bottom: time evolution of the temperature (blue) and the fuel mass fraction (red) at the leading edge position.

tion than before and, thus, reach it (and also richer mixtures zones) with more energy, successfully igniting the mixture and stabilising a new flame. This last observation shows that the increase in staging factor reduces the upstream motion of the stoichiometric zone, as the increase in magnitude of negative axial velocity that pushed the flame upstream also pushes the rich mixture upstream. Again, the bottom part of Fig. 6 confirms these results, showing that just before the increase in temperature caused by the consistent ignition and attachment of the pilot flame, the leading edge reaches the stoichiometric region and moves further upstream to richer mixture zones.

4. Conclusions

This work studied with high-fidelity LES the flashback and transition of a lean premixed M flame in a staged liquid-fuelled lean-burner, as observed experimentally in [4]. First, it is shown that the LPP $\alpha = 15\%$ M flame presents a strong acoustic activity, which creates a periodic temporary flashback of its leading edge. However, when the staging factor is increased to $\alpha = 20\%$, increasing the pilot injection in a manoeuvre that should stabilise the burner dynamics, the flame leading edge not only flashbacks, but reattaches at the pilot spray, changing the flame into a Tulip shape. Two phenomena were identified as being the most relevant ones controlling this flame shape transition: the final temperature of the combustion chamber and the injection regime.

The temperature of the combustion chamber impacts the M flame in two ways. First, it controls the stable axial position of the leading edge. The M flame being completely aerodynamically stabilised by a Bubble Vortex Breakdown and the CRZ bubble being filled with fresh cold air, the leading edge of the M flame stabilises behind the bubble at the threshold of the hot burnt gases. Therefore, the higher the final equilibrium burnt gases temperature and, thus, the more upstream the leading edge is stabilised. This effect was seen here by changing the heat losses at the chamber walls, which modified the final temperature in the chamber and, thus the stable position of the M flame leading edge. Second, as this is a combustion-instability-induced flashback, the higher the combustion chamber temperature, the higher the acoustic oscillations, which creates periodic flashbacks of the leading edge and contributes to increase the distance travelled by it.

However, the reattachment of the flame, and thus the flame transition, only occurs when, additionally to a sufficiently high temperature inside the chamber, the pilot injection attains a certain level. Increasing the pilot injection fuel mass flow rate increases the distance where the spray-created fuel rich zone penetrates inside the divergent. This allows the periodic flashback of the leading edge to reach and ignite this fuel rich zone, re-creating the flame root and making the flame transition into a Tulip shape.

Finally, this work provided insights that can be generalised and some control parameters that can be

manipulated for a safer operation of LPP M flames. First, as the flashback of the M flame leading edge is intrinsic to high acoustic activity, the suppression of any acoustic feedback is critical. However, even in the absence of self-sustained thermoacoustic oscillations in the chamber this transition could be triggered if the final temperature inside the chamber is high enough to put the leading edge of the M flame too close of the pilot spray. Thus, the final equilibrium temperature must be controlled (by regulating the global equivalence ratio, for example) to place the M flame leading edge sufficiently downstream of the injection systems. Lastly, one can prevent this flame shape transition by avoiding the leading edge to reach the pilot spray. This implies two possible design paths for this staged LPP burner: either this injector requires a different flow topology to operate with an M lifted flame, where the Central Recirculation Zone does not connect the flame to the pilot injector, or another flame shape should be used. As increasing the staging factor does not represent an increase in stability for the M lifted flame (which is the objective of staged injection [3]), but rather the use of the pilot injection represents a major risk for the M flame operation, it seems that the M lifted flame is not adapted to staged burners, and another flame shape, possibly attached or stabilised over the ISL without a lifted leading edge, could respond better to the multiple injection regimes of staged burners and offer more benefits for this type of combustor.

Acknowledgments

We thank CERFACS for sharing the AVBP solver. This work was granted access to the HPC resources of CINES under the allocation A0012B00164 made available by GENCI, and of the mesocentre computing center of CentraleSupélec and Ecole Normale Supérieure Paris-Saclay supported by CNRS and Region Ile-de-France (http://mesocentre.centralesupelec.fr/). We finally thank CentraleSupélec and Université Paris-Saclay for Léo's Ph.D. grant.

References

[1] S. Ducruix, T. Schuller, D. Durox, S. Candel, Combustion dynamics and instabilities: Elementary coupling and driving mechanisms, Journal of Propulsion and Power 19 (5) (2003) 722–734.

[2] T. C. Lieuwen, Unsteady Combustor Physics, Cambridge University Press, 2012. doi:10.1017/CBO9781139059961.

[3] Y. Huang, V. Yang, Dynamics and stability of lean-premixed swirl-stabilized combustion, Progress in Energy and Combustion Science 35 (4) (2009) 293–364.

[4] A. Renaud, S. Ducruix, P. Scouflaire, L. Zimmer, Flame shape transition in a swirl stabilised liquid fueled burner, Proceedings of the Combustion Institute 35 (2015) 3365–3372.

[5] L. C. C. Mesquita, A. Vié, S. Ducruix, LES of the Ignition of a Two-Phase Staged Swirling Burner: Influence of Ignition Location and Operating Conditions on the Flame Shape, in: Turbo Expo: Power for Land, Sea, and Air, Vol. Volume 4A: Combustion, Fuels, and Emissions, 2020. doi:10.1115/GT2020-15227.

[6] A. Renaud, S. Ducruix, L. Zimmer, Bistable behaviour and thermo-acoustic instability triggering in a gas turbine model combustor, Proceedings of the Combustion Institute 36 (2017) 3899–3906.

[7] L. C. Mesquita, A. Vié, L. Zimmer, S. Ducruix, Numerical analysis of flame shape bifurcation in a two-stage swirled liquid burner using large eddy simulation, Proceedings of the Combustion Institute 38 (4) (2021) 5971–5978. doi:https://doi.org/10.1016/j.proci.2020.06.044.
URL https://www.sciencedirect.com/science/article/pii/S154

[8] S. Hermeth, G. Staffelbach, L. Y. Gicquel, V. Anisimov, C. Cirigliano, T. Poinsot, Bistable swirled flames and influence on flame transfer functions, Combustion and Flame (2013). doi:10.1016/j.combustflame.2013.07.022.

[9] C. J. Lapeyre, M. Mazur, P. Scouflaire, F. Richecoeur, S. Ducruix, T. Poinsot, Acoustically Induced Flashback in a Staged Swirl-Stabilized Combustor, Flow, Turbulence and Combustion 98 (1) (2017) 265–282. doi:10.1007/s10494-016-9745-2.

[10] P. Wolf, R. Balakrishnan, G. Staffelbach, L. Gicquel, T. Poinsot, Using LES to study reacting flows and instabilities in annular combustion chambers, Flow, Turbulence and Combustion 88 (1) (2012) 191–206.

[11] F. Nicoud, F. Ducros, Subgrid-scale stress modelling based on the square of the velocity gradient tensor, Flow, Turbulence and Combustion 62 (3) (1999) 183–200.

[12] T. Poinsot, S. Lele, Boundary conditions for direct simulations of compressible viscous flows, Journal of Computational Physics 101(1) (1992) 104–129.

[13] B. Abramzon, W. Sirignano, Droplet vaporization model for spray combustion calculations, International Journal of Heat Mass Transfer 32 (1989) 1605–1618.

[14] L. C. C. Mesquita, A. Vié, S. Ducruix, Large eddy simulations of a two-phase staged swirling burner using an euler-lagrange approach: validation of the injection strategy. GT2018-76125, in: Proceedings of the ASME Turbo Expo 2018, Oslo, Norway, 2018.

[15] B. Franzelli, E. Riber, M. Sanjosé, T. Poinsot, A two-step chemical scheme for kerosene–air premixed flames, Combustion and Flame 157 (7) (2010) 1364 – 1373.

[16] P. Poinsot, D. Veynante, Theoretical and Numerical Combustion, CERFACS, Third Edition, 2012.

[17] F. Charlette, C. Meneveau, D. Veynante, A power-law flame wrinkling model for LES of premixed turbulent combustion part II: dynamic formulation, Combustion and Flame 131 (1–2) (2002) 181 – 197.

[18] A. Lefebvre, D. Ballal, Gas Turbine Combustion (3rd Edition), Taylor and Francis, Philadelphia, USA, 2010.

[19] O. Lucca-Negro, T. O'Doherty, Vortex breakdown: a review, Progress in Energy and Combustion Science 27 (2001) 431–481.

[20] A. C. Benim, K. J. Syed, Flashback Mechanisms in Lean Premixed Gas Turbine Combustion, Academic Press, 2015. doi:10.1016/B978-0-12-800755-6.00018-0.

[21] S. Candel, D. Durox, T. Schuller, J. Bourgouin, J. P. Moeck, Dynamics of swirling flames, Annual Reviews of Fluid Mechanics 46 (2014) 147–76.